IBIS
BOU international journal of avian science
Ibis (2021), **163**, 448–462 doi: 10.1111/ibi.12890

Discovery of a morphologically and genetically distinct population of Black-tailed Godwits in the East Asian-Australasian Flyway

BING-RUN ZHU,[1,2] YVONNE I. VERKUIL,[2] JESSE R. CONKLIN,[2] AILIN YANG,[1] WEIPAN LEI,[1] JOSÉ A. ALVES,[3,4] CHRIS J. HASSELL,[5] DMITRY DOROFEEV,[6] ZHENGWANG ZHANG[1]* & THEUNIS PIERSMA[2,5,7,8]

[1]*Key Laboratory for Biodiversity Science and Ecological Engineering, College of Life Sciences, Beijing Normal University, Beijing, 100875, China*

[2]*Conservation Ecology Group, Groningen Institute for Evolutionary Life Sciences, University of Groningen, PO Box 11103, Groningen, 9700 CC, The Netherlands*

[3]*Department of Biology and CESAM, Centre for Environmental and Marine Studies, University of Aveiro, Campus de Santiago, Aveiro, 3810-193, Portugal*

[4]*South Iceland Research Centre, University of Iceland, Lindarbraut 4, Laugarvatn, IS-840, Iceland*

[5]*Global Flyway Network, Australasian Wader Studies Group, PO Box 101 Curtin, ACT 2605, Broome, WA, 6725, Australia*

[6]*All-Russian Research Institute for Environmental Protection, 36 km MKAD 1 str 4, Moscow, 117628, Russia*

[7]*Department of Coastal Systems, NIOZ Royal Netherlands Institute for Sea Research, Utrecht University, PO Box 59, Texel, 1790 AB Den Burg, The Netherlands*

[8]*CEAAF Center for East Asian-Australasian Flyway Studies, Beijing Forestry University, Qinghua East Road 35, Haidian District, Beijing, 100083, China*

Occurring across Eurasia, the Black-tailed Godwit *Limosa limosa* has three recognized subspecies, *melanuroides*, *limosa* and *islandica* from east to west, respectively. With the smallest body size, *melanuroides* has been considered the only subspecies in the East Asian-Australasian Flyway. Yet, observations along the Chinese coast indicated the presence of distinctively large individuals. Here we compared the morphometrics of these larger birds captured in northern Bohai Bay, China, with those of the three known subspecies and explore the genetic population structuring of Black-tailed Godwits based on the control region of the mitochondrial genome (mtDNA). We found that the Bohai Godwits were indeed significantly larger than *melanuroides*, resembling *limosa* more than *islandica*, but with relatively longer bills than *islandica*. The level of genetic differentiation between Bohai Godwits and the three recognized subspecies was of similar magnitude to the differentiation among previously recognized subspecies. Based on these segregating morphological and genetic characteristics, we propose that these birds belong to a distinct population, which may be treated and described as a new subspecies.

Keywords: genetic population structure, migration, morphology, mtDNA, subspeciation, shorebirds, taxonomy.

Black-tailed Godwits *Limosa limosa* (hereafter, 'Godwits') breed across the Palaearctic (Engelmoer & Roselaar 1998, Gill *et al.*, 2007). Three subspecies have been described based on morphological and genetic traits: the nominate and widespread *L. l. limosa* Linnaeus, 1758, the Icelandic *L. l. islandica* C. L. Brehm, 1831 and the eastern *L. l. melanuroides* Gould, 1846 (Cramp & Simmons 1982, Höglund *et al.* 2009). The subspecies *islandica* breeds almost exclusively in Iceland, with a wide winter

*Corresponding author.
Email: zzw@bnu.edu.cn
Twitter: @DrewBingrun

distribution along the coasts of western Europe, and predominantly occupies estuarine habitats (Alves *et al.* 2013a), whereas *limosa* breeds primarily in western Europe but extends very far east, mainly using inland freshwater habitats in southwestern Europe and west Africa during the rest of the year (Kentie *et al.* 2017, Senner *et al.* 2019, Verhoeven *et al.* 2019). The distributional ranges and migratory flyways of the two European breeding subspecies partially overlap (Lourenço & Piersma 2008, Alves *et al.* 2010, 2013b, Hooijmeijer *et al.* 2014). The subspecies *melanuroides* has a breeding range that extends across eastern Russia, Mongolia and north China; during the non-breeding season, they are widely distributed across southeast Asia and extending to Australia (Groen *et al.* 2006, van Gils *et al.*, 2020).

The subspecies *limosa* is morphologically the largest of the three and increases in size across its distributional range from west to east (Prater *et al.* 1977). The smallest subspecies is *melanuroides*, which has a relatively short bill (Zhu *et al.* 2020). The subspecies *limosa* and *melanuroides* differ in size but not body shape, with *islandica* being smaller than *limosa* but with relatively long wings (Zhu *et al.* 2020). In addition, the breeding plumages of *melanuroides* and *islandica* are darker than in *limosa* (Groen & Yurlov 1999). For all three subspecies, females are the larger sex. Overlapping morphometrics between sexes and among subspecies prevents anonymous individuals from being assigned to subspecies based on body size measurements, but not on the basis of the maternally inherited mitochondrial DNA (mtDNA) (Lopes *et al.* 2013). With a high mutation rate, mtDNA provides information on recent differentiation within species (Avise 2000). Höglund *et al.* (2009), later confirmed by Trimbos *et al.* (2014), discovered three mitochondrial lineages using the control region (CR) of Black-tailed Godwits, with the three main haplotypes corresponding to the three recognized subspecies.

Although the small-bodied *melanuroides* was thought to be the only subspecies occurring in the East Asian-Australasian Flyway (EAAF), Engelmoer and Roselaar (1998) noted the presence in museum collections of large-sized Godwits collected along the Chinese coast (Shandong, Jiangsu and Fujian provinces) between 1900 and 1950. However, this was ascribed to geographical variation within *melanuroides*. Over the last decade, field observations of Godwits similar in size to *limosa* in eastern China, i.e. with rather long and thick bills and a paler plumage compared with the smaller co-occurring Godwits (thought to be *melanuroides*), have reopened the discussion. Such observations (A. Boyle & J. Allcock pers. comm., C.J.H. unpubl. data) were mainly made during spring at Bohai Bay in Tianjin City, Hebei Province,and in Shandong Province, both in China, between March and May (Fig. 1a), as well as between August and March in the Mai Po Wetland of Hong Kong (Fig. 1b; K. Leung pers. comm.). Interestingly, the thousands of individuals seen in the north of Bohai Bay in spring were nearly all of the larger Godwit type, with only a few hundred smaller ones seen after most large Godwits had left around mid-May (B.R.Z. 2014–2018, unpubl. data).

In this study, we examine the possibility that the large Black-tailed Godwits encountered along the coast of East Asia belong to a putative unrecognized population, with segregating differences that may warrant sub-specific status. We compare the morphometrics of molecularly sexed Godwits captured in northern Bohai Bay in China with breeding birds from Iceland and The Netherlands,

Figure 1. (a) Black-tailed Godwits foraging in Nanpu saltpan in April 2015. The one on the right represents the most common size in the Bohai Bay region; its height and bill length are distinct from the one on the left (Photo by B.R.Z.). (b) The wintering population of Black-tailed Godwits in Mai Po Wetland of Hong Kong in December 2016. The foremost one was strikingly smaller than the rest of the Godwits (photo by Qiuhe Chen).

and wintering birds in northwest Australia (assumed to belong to the three known subspecies *islandica*, *limosa* and *melanuroides*, respectively). We also analyse mtDNA of individuals sampled at the breeding, wintering or staging sites of the three known subspecies, together with individuals from Bohai Bay and associated sites, to provide the first phylogeographical assessment of the large birds from Bohai Bay. We conclude that the large birds represent a hitherto undescribed population of Black-tailed Godwit.

METHODS

Field observations were carried out along the northern shore of Bohai Bay (Fig. 2, 117.8–118.2°E, 39.0–39.2°N), in Nanpu County, Hebei Province, and at Hangu, Tianjin, China, from April to mid-May 2014–2018. We identified two major staging sites for Black-tailed Godwits. The first site, the Nanpu saltpans, is a 290-km^2 area that contains many shallow ponds for roosting and foraging waterbirds (Lei *et al.* 2018). The second site, the Hangu intertidal mudflats (117.9–118.0°E, 39.1–39.2°N), is located 20 km west of Nanpu. In addition, to the north of the Hangu mudflats, a shrimp farm of 5 km^2 was continually used by Godwits as a high-tide roost.

At Nanpu, Godwits were trapped during the day using spring-powered clap-nets (diameter of 150 cm) and noose-mats (Mehl *et al.* 2003) as they foraged. Traps were placed at frequently used pathways of Godwits along canals or along the edges of saltpans. At the Hangu inter-tidal mudflats, a large man-powered double clap-net (550 × 220 cm) was established on the first area of mudflat to be exposed after high tide. With many Godwits landing and the net camouflaged

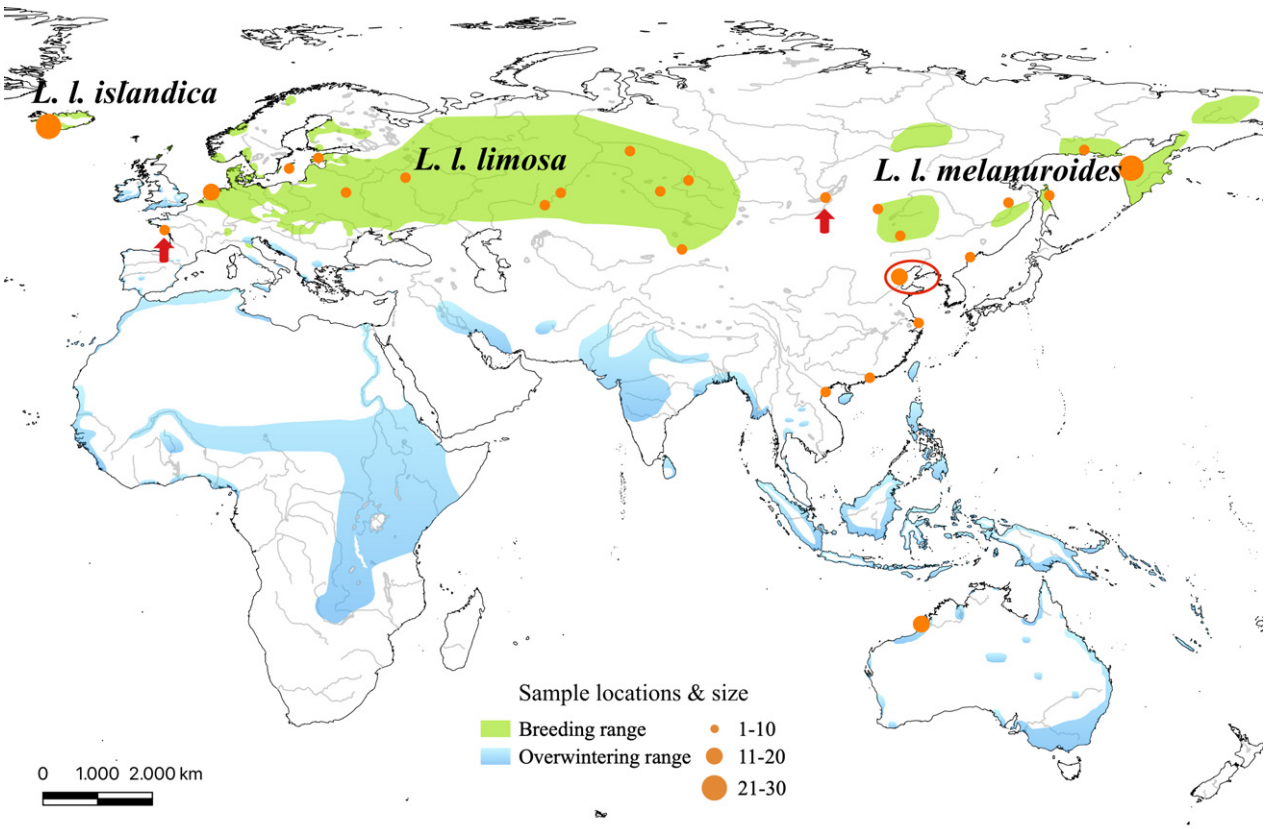

Figure 2. Study site in Bohai Bay (the red ellipse), sampling locations from which genetic samples were collected (solid circles) and the published breeding distributions of the three known subspecies of Black-tailed Godwits across Eurasia. The red arrows indicate one breeding location of *limosa* in France, and one breeding location of *melanuroides* in the Selenga Delta. Map created using QGIS 3.4.3 based on data in BirdLife International (2017).

by mud, we successfully made two catches. In the shrimp farm of Hangu, the ponds where the population was concentrated during high tide, mist-nets were also employed to sample birds at night from mid-April to the beginning of May.

Captured Godwits received a metal ring on the left tibia and were fitted with uniquely coded flags on the right tibia. The scheme followed the protocol on the EAAF (blue flag over the yellow flag on the tibia). The morphometric measurements were taken by a single observer (B.R.Z.) with age assigned on the basis of wear and colour of the primary feathers (Prater *et al.* 1977). Data for the three captured second calendar year birds were excluded from the present analysis. The length of the bill (culmen length), total head (head to bill), tarsus and tarsus to toe (tarsus plus mid-toe excluding the nail) were measured to the nearest 0.01 mm, and the flattened wing length was measured to the nearest 1 mm (Zhu *et al.* 2020). Additionally, we acquired these same measurements and tissue samples from fresh carcasses ($n = 8$) found at the two study sites. Causes of death included collisions with power lines and depredations. In the live birds, a blood sample of 20–60 μL was taken from the brachial vein and stored in 96% ethanol at −20 °C for subsequent molecular sexing and DNA analysis (further details in Velde *et al.* 2017). The banding work and collection of blood samples were approved by the Wild Animal and Plant Protection Division of the Forestry Department in Hebei, China.

Morphometric and molecular sexing data of *islandica*, *limosa* and *melanuroides* were obtained from two breeding sites in Iceland (65.67°N, −14.78°E, courtesy of T. G. Gunnarsson), The Netherlands (52.98°N, 5.4°E, courtesy of J. C. E. W. Hooijmeijer of the University of Groningen) and one wintering site in northwest Australia (17.94°S, 122.25°E, courtesy of the Global Flyway Network), respectively (Table S1). Morphology was previously analysed in Zhu *et al.* (2020). To compare the body dimensions of the Bohai Bay Black-tailed Godwits with the three known subspecies, we used analyses of variance (one-way analysis of variance (ANOVA)) and Tukey's honestly significant difference (HSD; Tukey 1949) tests. The degree of sexual size dimorphism (DSD) was calculated using the formula: $\left(\frac{\text{female mean body dimension}}{\text{male mean body dimension}} - 1\right)$, with values larger than zero indicating that females are larger than males (Lovich & Gibbons 1992). To compute the body size and shape for each population and both sexes of the three known subspecies and the Bohai Godwits, principal component analysis (PCA) was performed. To do this we used the R function *prcomp* with body dimensions (bill length, total head, tarsus, tarsus to toe and wing length; data were not transformed) as vectors; the analysis only includes individuals with complete sets of measurements. We constructed the biplot by the PC values in which more than 80% of the variation was represented. The first component of the *x*-axis (PC1) is generally interpreted as size, and the second component (PC2) of the *y*-axis as shape (Sundberg 1989, Zhu *et al.* 2020); the origin of the biplot was the average value of size or shape.

A collection of 240 blood and tissue samples of Black-tailed Godwits was assembled from 27 locations (Fig. 2 and Table S2). Samples of *islandica* and *limosa* were obtained from breeding sites (Table S2). As for the eastern population of Black-tailed Godwit, samples were gathered from various locations along the EAAF (Table S2). The blood samples taken for genotyping from the Bohai Godwits were from the same birds from which we collected morphometric data. For *islandica*, *limosa*, *melanuroides* and Godwits of unknown subspecies in the flyway, blood and tissue samples were collected by various colleagues, which did not always allow us to collect morphometric data from the same individuals. We used the ammonium acetate (AmAc) DNA extraction method (Richardson *et al.* 2001), followed by polymerase chain reaction (PCR) amplification with the sexing primer pair 2602F and 2669R (see van der Velde *et al.* 2017 for protocols). PCR products were visualized on a 2% agarose gel. Overall, 46 individuals (24 males and 22 females) from Bohai Bay were molecularly sexed, of which 12 samples were randomly picked to repeat the PCR step; the results were 100% consistent.

We developed nine PCR primers spanning the hypervariable Domain 1 of the mitochondrial CR and also the more conserved Domain 2 (Table S3). In Godwits, a site in Domain 2 has been shown to unambiguously discriminate between *islandica* and *limosa* (Lopes *et al.* 2013) and could be a generally informative site for identification of subspecies. Of all the combinations of primers, the primer sets L130 (the laboratory of GELIFES, University of Groningen) and H772 (Wenink *et al.*

1994) worked for samples from all putative populations. This primer pair was used to sequence a 642-bp CR fragment for all samples. Each PCR consisted of 1 μL extracted DNA, 4.16 μL ddH_2O, 10× buffer (100 mM Tris HCl, pH 8.8, 500 mM KCl, 1% Triton X-100), 1.28 μL dNTPs, 0.5 μL $MgCl_2$, 0.06 μL Taq (Promega, Madison, WI, USA) and 1 μL of each primer (L130: 5′-ACTTCCAACCGGGCAATACC-3′, H772: 5′-AAACACTTGAAACCGTCTCAT-3′). Cycling was performed with the following reaction conditions: initial denaturation at 94 °C for 1 min, 30 cycles of 30 s at 94 °C, 1 min at 54 °C, 2 min at 72 °C, and final elongation at 72 °C for 10 min. Samples were then purified following the SAPEXO enzymatic PCR cleanup protocol. Lastly, PCR products were subjected to ABI Sanger sequencing with both forward and reversed complements to obtain overlapping forward and reverse sequences for each sample.

For each sample, a pairwise alignment of the forward and reverse sequence was created, which was edited using the base-call quality information of the electropherogram to obtain a consensus sequence of the overlapping areas with unambiguous bases. Editing was performed blindly, meaning the sequence ID did not reveal the sampling location, using GENEIOUS 8.1.9 (Auckland, New Zealand). Subsequently, we named each consensus sequence after the field sample name and sampling location to facilitate hypothesis-driven analyses. To determine the haplotypes and their frequency of occurrence in our samples and to calculate genetic diversity in mtDNA, we used DNASP v 5.0 (Librado & Rozas 2009). In the analyses, invariable sites were included, and gaps were considered to contribute to the haplotypic variation. The package *Pegas* in R v 3.6.0 was used to visualize the haplotype network.

Next, we assigned all the samples to four putative population clusters corresponding to three known subspecies and the putative population of the Bohai Godwits. These hypothetical populations were inferred on the basis of the known distributions of Godwits and the mtDNA haplotype networks. The mtDNA haplotype network indicated that the samples from Shanghai were distributed over two distinct haplotype clusters. Our field observations and ringing data (B.R.Z. 2014–2018 unpubl. data) also confirmed that during the staging period, this site was used both by the 'large' and 'small' Godwits, the latter probably representing *melanuroides*. Unfortunately, for five of the birds from Shanghai, the mtDNA data were not matched with individuals from which morphological data were collected. Hence, in subsequent analyses we excluded the seven samples from Shanghai. One Icelandic sample appeared in the haplotype cluster comprising the *limosa* samples (this was also observed by Trimbos *et al.* 2014). As this sample was collected during the breeding season in Iceland, we considered this placement in the *limosa* cluster to be a consequence of potential gene flow. Thus, this individual was kept in the *limosa* group for subsequent analyses.

To infer the evolutionary relationships among populations, we only included haplotypes represented by more than 18 individuals (range: 18–42). We constructed a neighbour-joining phylogenetic tree in GENEIOUS 8.1.9 with the Bar-tailed Godwit *Limosa lapponica* as an outgroup (GenBank accession number AY524807.1; X. Wang, Y. Sun and Q.-W. Li unpubl. data), using the Tamura–Nei genetic distance model with 1000 bootstrap iterations. Finally, population pairwise F_{st} tests (Tajima & Nei 1984) and an analysis of molecular variance (AMOVA, Excoffier *et al.* 1992) were performed to estimate the genetic differentiation between each haplotype/putative population (ARLEQUIN 1.1.; Schneider *et al.* 1997).

RESULTS

Morphology

Black-tailed Godwits from Bohai Bay were significantly larger than *melanuroides* in all body dimensions for both sexes (Table S4, Fig. 3a–e). Female Bohai Godwits were larger than males, and the degree of sexual dimorphism was greatest for bill length and least for wing length, a pattern consistent with the three recognized subspecies (Table S4).

A PCA of the body dimensions for the two Asian populations showed that *melanuroides* and the Bohai Godwits represented two separate clusters (Fig. 3f). The body size of the Bohai Godwits was more similar to that of *limosa* than to the smaller *islandica* and *melanuroides*. The first two principal components explained 94% (Table 1, Fig. 4) of the variance (87.2 and 6.4% for PC1 and PC2, respectively). All vectors of body dimensions were highly correlated with each other. The vectors of sex pointed in opposite directions along

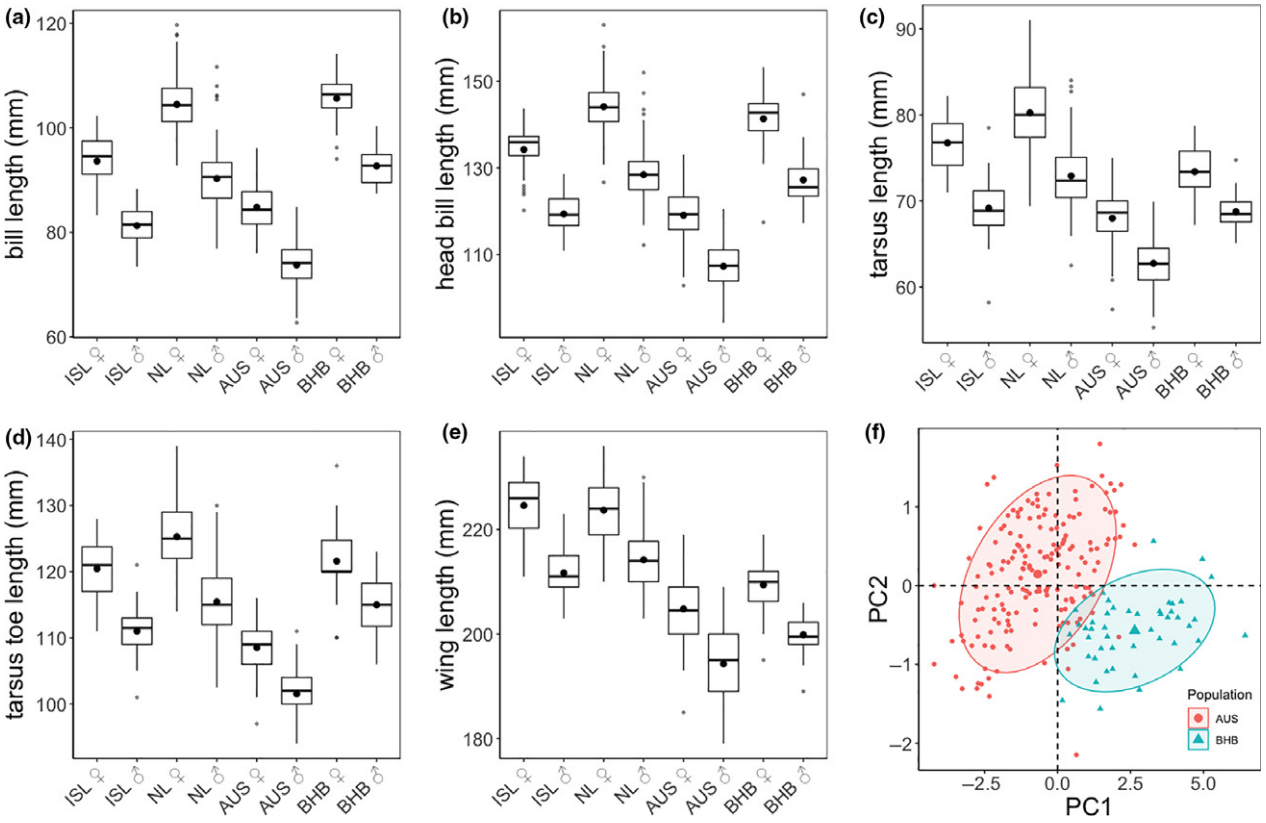

Figure 3. (a–e) The bill, total head, tarsus, tarsus–toe and wing length of female (♀) and male (♂) Black-tailed Godwits from Iceland (ISL, *L. l. islandica*), The Netherlands (NL, *L. l. limosa*), NW Australia (AUS, *L. l. melanuroides*) and Bohai Bay (BHB); horizontal lines within boxes represent the median, and dots represent mean values. (f) A PCA of morphometrics from Bohai Bay and northwest Australia; the ellipses were constructed with a 95% confidence interval. [Colour figure can be viewed at wileyonlinelibrary.com]

the *x*-axis, meaning that males were smaller than females in overall body size. The projection of *melanuroides* on the far left of the *x*-axis (PC1) indicated the smallest body size; on the far right of the *x*-axis, *limosa* was the largest, with *islandica* and the Bohai Godwits falling in between. The Icelandic Godwits were only slightly smaller than the Godwits from Bohai Bay. The projection of the four populations on the *y*-axis (PC2; Fig. 4) indicated that *islandica* and the Bohai Godwits aligned on the same axis of body shape but were different from *limosa* and *melanuroides*, which only differ in size.

Table 1. Eigenvalues and cumulative percentage of PCA of Black-tailed Godwits, using body dimensions (length of the bill, total head, tarsus, tarsus to toe, wing) as vectors.

	PC1	PC2	PC3	PC4	PC5
Eigenvalues	4.36	0.32	0.23	0.06	0.03
% of variance	87.15	6.35	4.60	1.26	0.63
Cumulative % of variance	87.15	93.51	98.11	99.37	100.00

PC1 and PC2 explained 93.5% of the cumulative percentage of variance.

Genetic differentiation

Unambiguous consensus sequences of 482 bp of the mtDNA CR were obtained for 195 individuals (GenBank accession numbers MT302861–MT303055). Thirty-six mtDNA haplotypes were identified among 27 sampling locations (Table S2). Five haplotypes were common (found in 18–42 individuals each); overall genetic diversity was 0.90. Four haplotype clusters could be distinguished (Fig. 5). Haplotype cluster I encompassed 27 of 28 samples from Iceland where *islandica* breeds. Haplotype cluster II encompassed

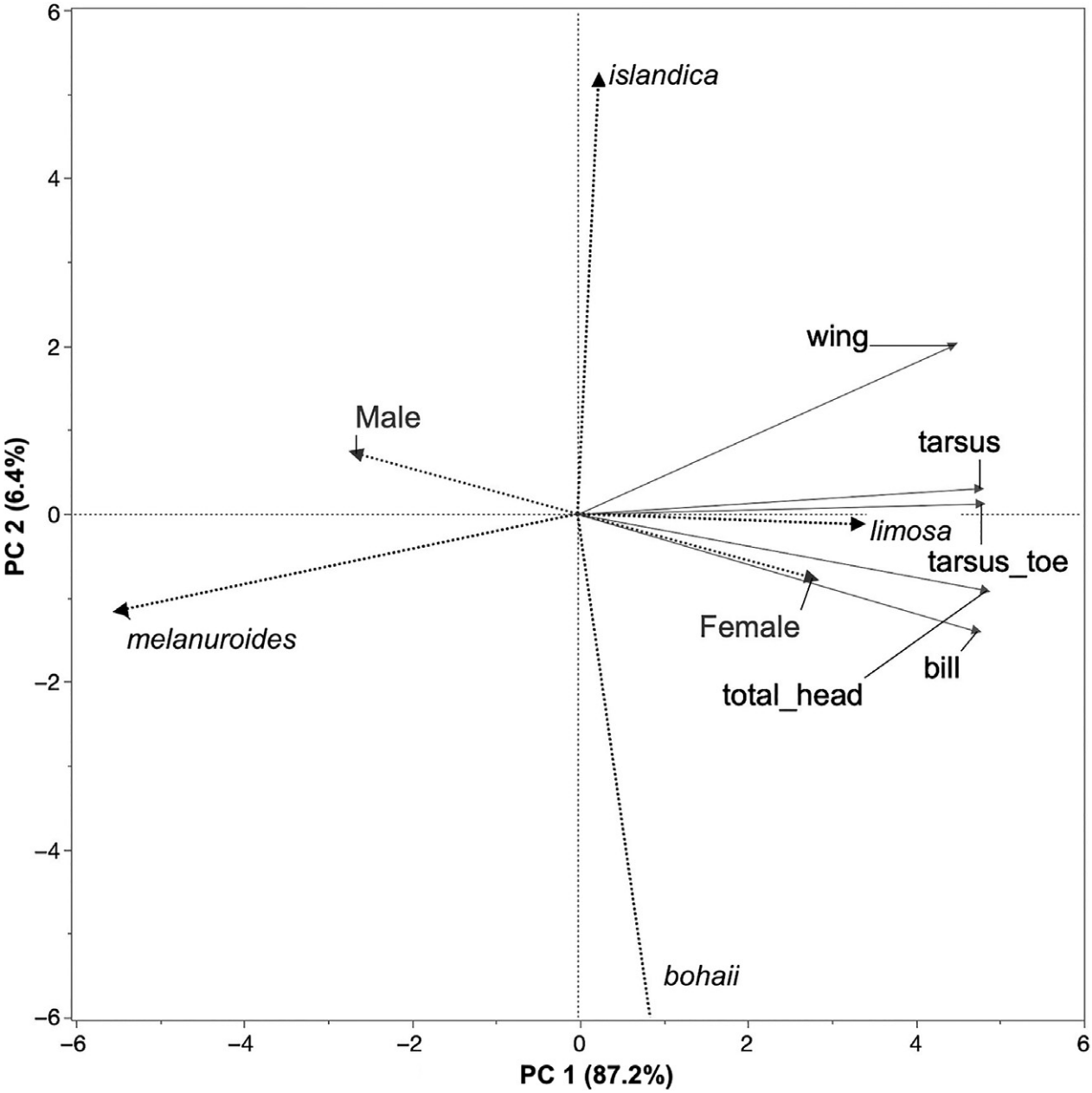

Figure 4. PCA correlation of linear dimensions (bill length, total head, tarsus, tarsus to toe, wing) with sex and subspecies as explanatory variables.

individuals sampled at locations from France to Altai Krai in Russia, which is the breeding range of *limosa*, and included one individual from Iceland (bk306, Fig. 5, Table S5). Note that the two common haplotypes in this cluster did not correspond with the eastern to western geographical distribution of *limosa* but were intermixed. Haplotype cluster III included all samples from Bohai Bay, Hong Kong, Vietnam and one Shanghai sample. Haplotype cluster IV included samples from the breeding range of *melanuroides* from the Selenga Delta of Russia eastward, including Inner Mongolia of China, as well as the staging area in Shanghai, China ($n = 6$), and wintering range of *melanuroides* in northwest Australia.

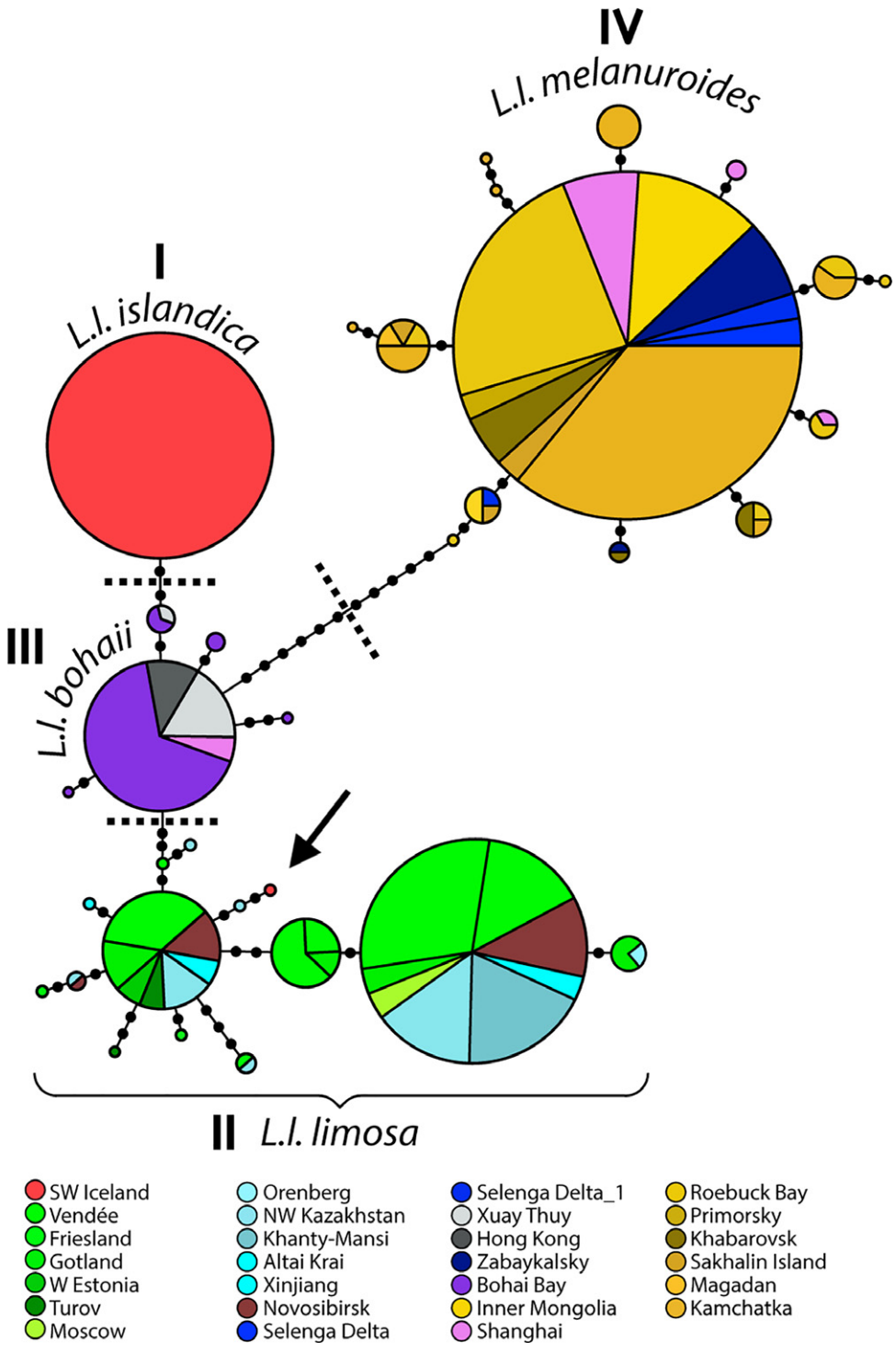

Figure 5. Mitochondrial DNA haplotype networks of the three known subspecies and the Bohai Bay Black-tailed Godwits. Each pie chart represents a unique haplotype; the size of the pie indicates the sample size of the haplotype; the colours show the sample locations; and each dot through the line between haplotypes is one mutational step. The arrow indicates one Icelandic sample (bk306) that clustered with the *limosa* haplotype.

The common haplotype in cluster III (all belonging to the Bohai population) differed from the common haplotype in cluster I (*islandica*) by four mutations, and by four and nine mutations from the common haplotypes in clusters II and III (*limosa*), respectively. As many as 15 mutations separated the common haplotype of cluster IV (*melanuroides*) from cluster III (Fig. 5). The neighbour-joining phylogenetic tree suggested that *melanuroides* represented the oldest branch, followed by a major split into two 'sister' branches, one of which included both the *islandica* and the Bohai haplotypes, and the other all *limosa* haplotypes (Fig. S1). F_{st} values supported this result for pairwise population differentiation, yielding significant differentiation between all four clusters (Table 2). The highest level of genetic differentiation was observed between the Bohai Godwits and *melanuroides* ($F_{st} = 0.94$, $P < 0.0001$), then with *islandica* ($F_{st} = 0.80$, $P < 0.0001$) and *limosa* ($F_{st} = 0.60$, $P < 0.0001$), respectively. The variation among subspecies with the Bohali Godwits treated on their own was 90.67% and within subspecies/Bohali was 9.33% (Fixation Index = 0.90668, $P < 0.0001$, AMOVA).

DISCUSSION

Our study confirmed that a morphologically large population of Black-tailed Godwits shares the EAAF with the *melanuroides* subspecies (Table S4). In the single previous acknowledgement of the presence of large birds in this flyway (Engelmoer & Roselaar 1998), this was considered to reflect geographical variation within *melanuroides*. Genetic analyses revealed a distinct haplotype cluster for the large Godwits from Bohai Bay and similar birds from other non-breeding sites in the flyway (Fig. 5). Population pairwise F_{st} values indicated high levels of segregation (0.60–0.95) between the Bohai birds and the three described subspecies (Table 2).

Table 2. Population pairwise F_{st} among the three known subspecies and the hypothesized Bohai population of Black-tailed Godwits.

	islandica	*limosa*	Bohai	*melanuroides*
islandica	–	***	***	***
limosa	0.73	–	***	***
Bohai	0.80	0.60	–	***
melanuroides	0.95	0.92	0.94	–

Above the diagonal, *P*-value based on 100 permutations (***$P < 0.0001$); below the diagonal, values comparing each population to all others (distance method: Tajima & Nei 1984).

The mtDNA haplotype network recovered the divergence among the subspecies *melanuroides*, *islandica* and *limosa* reported by Högland *et al.* (2009) and Trimbos *et al.* (2014), both of whom used various genetic markers including the mitochondrial CR. We obtained lower node support in the neighbour-joining phylogenetic tree for the split between *islandica* and *limosa* (Fig. S1) compared with Trimbos *et al.* (2014). The probable reason for this difference is that Trimbos *et al.* (2014) sequenced the highly variable Domains 1 and 3 of the CRs, whereas we chose to sequence Domains 1 and 2 to ensure that we included the site that unambiguously segregates *islandica* and *limosa* (Lopes *et al.* 2013). However, Domain 2 is less variable (Wenink *et al.* 1993). Thus, although the haplotype network clearly segregates the subspecies, the dataset contains fewer mutations, which affects the node support values.

Our genetic results confirm the understood geographical boundary between the breeding ranges of *limosa* and *melanuroides*. As suggested by previous morphometric analyses (Engelmoer & Roselaar 1998) and genetic studies (Högland *et al.* 2009, Trimbos *et al.* 2014), the turnover in subspecies occurs in central Russia somewhere east of longitude 84°E and west of the Baikal region at 106°E. Furthermore, we now shed light on an unexpected finding by Elbourne (2011), who tested the strength of the mitochondrial cytochrome oxidase I (COI) barcoding gene (typically a species-level marker) to detect sub-specific structure in Black-tailed Godwits. She found an unexplained structure within *melanuroides* in which samples from Australia and the Russian Far East formed a cluster strongly differentiated from the other subspecies, and samples from Vietnam clustered separately from other *melanuroides* and much closer to *limosa*. Our haplotype network based on the mitochondrial CR showed that all three samples from Vietnam (including two of the same samples used in the COI study) were clustered with the Bohai Godwits (Fig. 5), explaining the results of Elbourne (2011) and suggesting that these two populations have distinct non-breeding distributions.

Intriguingly, Elbourne (2011) also found that two samples from the Selenga Delta did not

cluster together at the COI locus, one grouping with the Vietnam individuals and the other with the expected *melanuroides* individuals. She speculated that this might represent present-day contact between the two groups. We were unable to replicate this result, as all three Selenga samples in our final dataset (by chance including neither sample used by Elbourne) clustered with *melanuroides* (Fig. 5). However, the COI results might indicate: (1) that both populations breed in the Selenga region, (2) that some level of genetic introgression has occurred in the past or (3) that the samples collected there are not from breeding individuals. The Selenga delta is known as both a breeding and a passage area for Godwits (Fefelov & Tupitsyn 2004, Groen *et al.* 2006). Individual tracking or further genetic work will be required to describe whether and how Bohai Godwits use this region.

Previous morphological and molecular studies on sub-speciation of Black-tailed Godwits (Engelmoer & Roselaar 1998) did not have sufficient sampling to identify the 'Bohai' population. In this study, with broader coverage of sampling locations throughout the entire breeding range as well as samples from several key stopover sites, breeding and wintering locations in the EAAF, we were able to uncover this population. Owing to the distinct morphological and genetic characteristics, and the potential isolation of breeding and wintering ranges of Godwits sampled in Bohai Bay and associated sites, we suggest this population should be considered a hitherto undescribed subspecies, new to science. These results suggest that this newly recognized population warrants subspecies status (see formal description below).

Among the nine major global flyways, the EAAF has the highest diversity of migratory waterbird species and the highest percentage of declining waterbird populations (Delany *et al.* 2010). At the bottleneck of the flyway, the Bohai Sea is surrounded by one of the most populated and industrialized regions of China. It experiences very high pollution levels (Gao & Chen 2012) and loss of ecosystems due to land claims (Conklin *et al.* 2014, Ma *et al.* 2014, Melville *et al.* 2016, Piersma *et al.* 2016). On the other hand, Bohai Bay is crucial for many waterbird species and is used annually as a staging area by more than 1% of the flyway population of Black-tailed Godwits (Lei *et al.* 2018). At the species level, Black-tailed Godwits are declining and considered Near-Threatened on the global Red List (BirdLife 2017). We demonstrate that the current understanding of the seasonal distribution and population-size estimates for the 'eastern Godwits' has been based on a combination of *melanuroides* and the 'Bohai' population. A re-evaluation of the eastern Black-tailed Godwit populations will provide the continuing support to maintain and extend the ban on coastal reclamation in China (Chinese Government 2018), and the filling of knowledge gaps, particularly the identification of the spatial and temporal distributions of the two populations in the flyway, for example by satellite tracking (Chan *et al.*, 2019, Zhu, *et al.* 2020), should now receive priority.

Limosa limosa bohaii subspecies nov

Holotype

Specimen no. BNU-10098, Zoological and Botanical Museum of the Beijing Normal University, China, preserved as a study skin: adult female collected on 16 April 2018 at Hangu, Tianjin, China, by Bing-Run Zhu (Fig. 6a,c). This bird is unlikely to have shown full development of the alternate plumage (compared with the *limosa* subspecies; Schroeder *et al.* 2008, 2009).

Description of holotype

Forehead, crown, nape and ear coverts 70% French Grey. Chin 20% French Grey. Supercilium 10% French Grey. Eye stripes 50% French Grey. Mantle and back Sepia. Wing coverts between Light Umber and 90% French Grey with 20% French Grey edges. Primaries, secondaries and axillaries Dark Umber, tertials 70% French Grey. Rump, upper tail coverts and base of tail between Light Umber and 10% French Grey, and distal tail Black with 50% French Grey tail tip. Throat to foreneck 40% French Grey. Chest French 40% Grey with Bronze and Dark Brown bars. Belly and flanks between Light Umber and 5% French Grey. Vent 10% Warm Grey. Undertail coverts 30% French Grey. Bill 102.2 mm, tarsus 78.3 mm, wing 218 mm (colour coding references: Prismacolor).

Paratype

Specimen no. BNU-10099, Zoological and Botanical Museum of the Beijing Normal University, China, preserved as a study skin: adult female collected on 18 April 2018 at Hangu, Tianjin, China, by Bing-Run Zhu (Fig. 6b,d).

Figure 6. Holotype (a, c) and paratype (b, d) of *Limosa limosa bohaii* subsp. nov. Upper, dorsal and lower ventral aspects.

Description of paratype

Forehead, crown between Light Umber and Sepia with 90% French Grey dots. Nape and ear coverts between Bronze and Light Umber. Chin 20% French Grey. Supercilium 10% French Grey. Eye stripes Sepia. Mantle and back between Light

Umber and Sepia, some mantle feathers Ginger Root with Sepia fringes. Wing coverts between 30 and 50% French Grey with 10% French Grey edges. Primaries, secondaries and axillaries Dark Umber, and tertials 70% French Grey. Rump, upper tail coverts and base of tail between Light Umber and 20% French Grey, and distal tail Black with 50% French Grey tail tip. Throat 20% French Grey. Foreneck and upper chest between Bronze and Light Umber with Dark Brown and Sepia bars and dots. Lower chest, belly and flanks between Beige, Ginger Root and 10% French Grey with Dark Brown bars. Vent 10% Warm Grey. Undertail coverts 30% French Grey. Bill 101.7 mm, tarsus 80.2 mm, wing 218 mm.

Etymology

The chosen scientific name refers to the area in China (Bohai) where the story of this subspecies unfolded. The finding of this new subspecies of the Black-tailed Godwit in the EAAF will hopefully raise awareness for the conservation of migratory birds and wetlands in China.

Diagnosis

Significantly larger than *L. l. melanuroides* on each examined dimension. Bill length: *bohaii* ♀106 ± 5 mm, ♂93 ± 3 mm; *melanuroides* ♀85 ± 5 mm, ♂74 ± 4 mm. Total head length: *bohaii* ♀141 ± 8 mm, ♂ 127 ± 6 mm; *melanuroides* ♀119 ± 6 mm, ♂107 ± 5 mm. Tarsus length: *bohaii* ♀73 ± 3 mm, ♂69 ± 2 mm; *melanuroides* ♀68 ± 3 mm, ♂63 ± 3 mm. Tarsus toe length: *bohaii* ♀122 ± 6 mm, ♂115 ± 4 mm; *melanuroides* ♀109 ± 4 mm, ♂102 ± 3 mm. Wing length: *bohaii* ♀209 ± 6 mm, ♂200 ± 4 mm; *melanuroides* ♀205 ± 6 mm, ♂194 ± 7 mm.

Body size resembles *L. l. limosa* with a possibly lighter alternate plumage, but wing length is shorter than in *islandica* and *limosa* in both sexes: *bohaii* ♀209 ± 6 mm, ♂200 ± 4 mm; *islandica* ♀224 ± 6 mm, ♂214 ± 6 mm; *limosa* ♀225 ± 6 mm, ♂212 ± 6 mm.

Distribution

The new subspecies *bohaii* probably breeds in the Russian Far East. Based on the breeding range of the eastern Godwits population within the EAAF, only two locations in the Russian Far East were not covered by our study (Fig. 2). One is Chukotka, while the other is the central part of Sakha Republic. The morphological data from Chukotka suggested the occurrence of *melanuroides* (Engelmoer & Roselaar 1998). Hence, Sakha Republic is more likely to be the breeding ground of *bohaii*. In the non-breeding season, sightings were reported in Hong Kong, Vietnam (B.R.Z. 2014–2018, unpubl. data), Thailand (Chengxin Yu pers. comm.) and Malaysia (John Howes pers. comm.).

We thank all the volunteers (Hung-Ju Lin, Jianyu Liu, Mu Su, Guofu Li, Jinghui Lin, Sijia Pan), colleagues from Beijing Normal University and the Global Flyway Network (Pinjia Que, Jin Liu, Jianzhi Zhang, Yinong Liu, Yang Wu, Ziwen Chai, Qi Lu, Fuxing Wu, Adrian Boyle, Matt Slaymaker and Bob Loos) who joined or offered their help to the 'Godwit fieldwork' in Bohai Bay and Inner Mongolia, China. We thank Shifu Guo, Jan Visser, Abad-Gómez José, Qingshan Ma, Jianmin Wang and Zhiwei Tian for their great support with catching and taking care of Godwits. We thank Qiang Ma (Chongming Dongtan Birds National Nature Reserve), Katherine Leung and John Allcock (Hong Kong Mai Po Wetlands) for sharing the morphological data. We thank Mo Verhoeven and Jelle Loonstra for helping with analyses. We thank Xuan Li for helping with uploading the sequences to GenBank. We thank Dongsheng Guo for specimen preparation. We thank Lisa Sanchez-Aguilar for helping with the modification of the figures and code coloration of the holotype and paratype. We thank Prof. Zhijun Ma, Pavel Tomkovich, Pavel Pinchuk, Jacob Höglund, Krijn Trimbos, Frederic Robin of the University of Washington Burke Museum, the Royal Ontario Museum and the Yale Peabody Museum of Natural History for making tissue samples available. This research was funded by the Natural Science Foundation of China (31572288, 31830089), the National Geographic 'Air and Water Conservation' Fund (GEFC-02-16), SEE Foundation, the Netherlands Organization for Scientific Research (NWO), NERC (NE/H008527/1), the Icelandic Research Fund (130412-051), Fundação para a Ciência e a Tecnologia (FTC), with contributions from WWF-Netherlands and the Spinoza Premium 2014 of NWO Netherlands Organization for Scientific Research to T.P. to maintain the research activities of the Global Flyway Network in Northwest Australia. We are grateful to Nigel Clark, Rauri Bowie and an anonymous referee who contributed greatly to the improvement of the manuscript.

AUTHOR CONTRIBUTIONS

Bing-run Zhu: Conceptualization (lead); Data curation (lead); Formal analysis (lead); Funding acquisition (supporting); Investigation (lead); Methodology (lead); Project administration (lead);

Resources (lead); Software (lead); Visualization (lead); Writing-original draft (lead); Writing-review & editing (lead). **Yvonne Ingje Verkuil:** Conceptualization (supporting); Formal analysis (supporting); Methodology (supporting); Resources (supporting); Software (supporting); Writing-review & editing (supporting). **Jesse Conklin:** Conceptualization (supporting); Methodology (supporting); Resources (equal); Writing-review & editing (supporting). **Ailin Yang:** Methodology (supporting). **Weipan Lei:** Methodology (supporting). **José A. Alves:** Resources (supporting). **Chris J. Hassell:** Conceptualization (supporting); Resources (supporting). **Dmitry Dorofeev:** Resources (supporting). **Zhengwang Zhang:** Funding acquisition (lead); Supervision (lead); Writing-review & editing (supporting). **Theunis Piersma:** Conceptualization (supporting); Funding acquisition (supporting); Resources (supporting); Supervision (lead); Writing-original draft (supporting); Writing-review & editing (lead).

DATA AVAILABILITY STATEMENT

Morphological data are available in Table S1. The genetic data are available in NCBI GenBank at https:// www.ncbi.nlm.nih.gov/genbank; see Table S5 for accession numbers MT302861–MT303055.

REFERENCES

Alves, J.A., Gunnarsson, T.G., Hayhow, D.B., Appleton, G.F., Potts, P.M., Sutherland, W.J. & Gill, J.A. 2013a. Costs, benefits, and fitness consequences of different migratory strategies. *Ecology* **94**: 11–17.

Alves, J.A., Gunnarsson, T.G., Potts, P.M., Sutherland, W.J. & Gill, J.A. 2013b. Sex-biases in distribution and resource use at different spatial scales in a migratory shorebird. *Ecol. Evol.* **3**: 1079–1090.

Alves, J.A., Lourenço, P.M., Piersma, T., Sutherland, W.J. & Gill, J.A. 2010. Population overlap and habitat segregation in wintering Black-tailed Godwits *Limosa limosa*. *Bird Study* **57**: 381–391.

Avise, J.C. 2000. *Phylogeography. The History and Formation of Species*. Cambridge: Harvard University Press.

BirdLife International 2017. *Limosa limosa (amended version of 2016 assessment)*. The IUCN Red List of Threatened Species 2017: e.T22693150A111611637. http://dx.doi.org/10.2305/IUCN.UK.2017-1.RLTS.T22693150A111611637.en.

Chan, Y.-C., Tibbitts, T.L., Lok, T., Hassell, C.J., Peng, H.-B., Ma, Z., Zhang, Z.W. & Piersma, T. 2019. Filling knowledge gaps in a threatened shorebird flyway through satellite tracking. *J. Appl. Ecol.* **56**: 2305–2315.

Chinese Government 2018. *The Notice of Strengthening Protection of Coastal Wetlands and Strict Control of Reclamation*. State Council. Viewed 2 April 2020, http://www.gov.cn/zhengce/content/2018-07/25/content_5309058.htmhttp://english.www.gov.cn/news/top_news/2018/01/18/content_281476017712430.htm.

Conklin, J.R., Verkuil, Y.I. & Smith, B.R. 2014. *Prioritizing Migratory Shorebirds for Conservation Action on the East Asian-Australasian Flyway*. Hong Kong: WWF-Hong Kong. https://eaaflyway.net/wp-content/uploads/2018/01/wwf_prioritization_finalpdf.pdf

Cramp, S. & Simmons, K.E.L. (eds) 1982. *The Birds of the Western Palearctic,* Vol. **2**. Oxford: Oxford University Press.

Delany, S., Nagy, S. & Davidson, N. 2010. *State of the World's Waterbirds*. Wageningen: Wetlands International.

Elbourne, R., 2011. *Master of Science thesis: COI barcoding of the shorebirds: rates of evolution and the identification of species*. Department of Ecology and Evolutionary Biology, University of Toronto.

Engelmoer, M. & Roselaar, C.S. 1998. *Geographical Variation in Waders*. Dordrecht: Kluwer. https://link.springer.com/book/10.1007/978-94-011-5016-3

Excoffier, L., Smouse, P.E. & Quattro, J.M. 1992. Analysis of molecular variance inferred from metric distances among DNA haplotypes: application to human mitochondrial DNA restriction data. *Genetics* **131**: 479–491.

Fefelov, I. & Tupitsyn, I. 2004. Waders of the Selenga delta, Lake Baikal, eastern Siberia. *Wader Study Group Bull.* **104**: 66–78.

Gao, X. & Chen, C.T.A. 2012. Heavy metal pollution status in surface sediments of the coastal Bohai Bay. *Water Res.* **6**: 1901–1911.

Gill, J.A., Langston, R.H., Alves, J.A., Atkinson, P.W., Bocher, P., Vieira, N.C., Crockford, N.J., Gélinaud, G., Groen, N., Gunnarsson, T.G., Hayhow, B., Hooijmeijer, J.C.E.W., Kentie, R., Kleijn, D., Lourenço, P.M., Masero, J.A., Meunier, F., Potts, P.M., Roodbergen, M., Schekkerman, H., Schroeder, J., Wymenga, E. & Piersma, T. 2007. Contrasting trends in two Black-tailed Godwit populations. *Wader Study Group Bull.* **114**: 43–50.

van Gils, J., Wiersma, P., Christie, D.A., Garcia, E.F.J. & Boesman, P. 2020. Black-tailed Godwit (*Limosa limosa*). In del Hoyo, J., Elliott, A., Sargatal, J., Christie, D.A. & de Juana, E. (eds) *Birds of the World version 1.0*. New York, NY: Cornell Lab of Ornithology. https://doi.org/10.2173/bow.bktgod.01

Groen, N., Mes, R., Fefelov, I. & Tupitsyn, I. 2006. Eastern Black-tailed Godwits *Limosa limosa melanuroides* in the Selenga delta, Lake Baikal, Siberia. *Wader Study Group Bull.* **110**: 48–53.

Groen, N. & Yurlov, A.K. 1999. Body dimensions and mass of breeding and Black-tailed Godwits (*Limosa l. limosa*): a comparison between a west Siberian and Dutch population. *J. Ornithol.* **140**: 73–79.

Gunnarsson, T.G., Gill, J.A., Goodacre, S.L., Gélinaud, G., Atkinson, P.W., Hewitt, G.M., Potts, P.M. & Sutherland, W.J. 2006. Sexing of Black-tailed Godwits *Limosa limosa islandica*: a comparison of behavioural, molecular, biometric and field-based techniques. *Bird Study* **53**: 193–198.

Höglund, J., Johansson, T., Beintema, A. & Schekkerman, H. 2009. Phylogeography of the Black-tailed Godwit *Limosa limosa*: substructuring revealed by mtDNA control region sequences. *J. Ornithol.* **150**: 45–53.

Hooijmeijer, J.C.E.W., Senner, N.R., Tibbitts, T.L., Gill, R.E., Douglas, D.C., Bruinzeel, L.W., Wymenga, E. &

Piersma, T. 2014. Post-breeding migration of Dutch-breeding Black-tailed Godwits: timing, routes, use of stopovers, and nonbreeding destinations. *Ardea* **101**: 141–152.

Kentie, R., Marquez-Ferrando, R., Figuerola, J., Gangoso, L., Hooijmeijer, J.C.E.W., Loonstra, A.H.J., Robin, F., Sarasa, M., Senner, N., Valkema, H., Verhoeven, M.A. & Piersma, T. 2017. Does wintering north or south of the Sahara correlate with timing and breeding performance in Black-tailed Godwits? *Ecol. Evol.* **7**: 2812–2820.

Lei, W., Masero, J.A., Piersma, T., Zhu, B., Yang, H.Y. & Zhang, Z. 2018. Alternative habitat: the importance of the Nanpu Saltpans for migratory waterbirds in the Chinese Yellow Sea. *Bird Conserv. Int.* **28**: 549–566.

Librado, P. & Rozas, J. 2009. DnaSP v5: a software for comprehensive analysis of DNA polymorphism data. *Bioinformatics* **25**: 1451–1452.

Lopes, R.J., Alves, J.A., Gill, J.A., Gunnarsson, T.G., Hooijmeijer, J.C.E.W., Lourenço, P.M., Masero, J.A., Piersma, T., Potts, P.M., Rabaçal, B., Reis, S., Sánchez-Guzman, J.M., Santiago-Quesada, F. & Villegas, A. 2013. Do different subspecies of Black-tailed Godwit *Limosa limosa* overlap in Iberian wintering and staging areas? Validation with genetic markers. *J. Ornithol.* **154**: 35–40.

Lourenço, P.M. & Piersma, T. 2008. Stopover ecology of Black-tailed Godwits *Limosa limosa limosa* in Portuguese rice fields: a guide on where to feed in winter. *Bird Study* **55**: 194–202.

Lovich, J.E. & Gibbons, J.W. 1992. A review of techniques for quantifying sexual size dimorphism. *Growth Dev. Ageing* **56**: 269–281.

Ma, Z., Melville, D.S., Liu, J., Chen, Y., Yang, H., Ren, W., Zhang, Z., Piersma, T. & Li, B. 2014. Rethinking China's new great wall. *Science* **346**: 912–914.

Mehl, K.R., Drake, K.L., Page, G.W., Sanzenbacher, P.M., Haig, S.M. & Thompson, J.E. 2003. Capture of breeding and wintering shorebirds with leg-hold noose-mats. *J. Field Ornithol.* **74**: 401–405.

Melville, D.S., Chen, Y. & Ma, Z. 2016. Shorebirds along the Yellow Sea coast of China face an uncertain future – a review of threats. *Emu* **116**: 100–110.

Piersma, T., Lok, T., Chen, Y., Hassell, C.J., Yang, H.-Y., Boyle, A., Slaymaker, M., Chan, Y.-C., Melville, D.S., Zhang, Z.-W. & Ma, Z. 2016. Simultaneous declines in summer survival of three shorebird species signals a flyway at risk. *J. Appl. Ecol.* **53**: 479–490.

Prater, A.J., Marchant, J.H. & Vuorinen, J. 1977. *Guide to the Identification and Aging of Holarctic Waders*. Thetford: British Trust for Ornithology.

Richardson, D.S., Jury, F.L., Blaakmeer, K., Komdeur, J. & Burke, T. 2001. Parentage assignment and extra-group paternity in a cooperative breeder: the Seychelles warbler (*Acrocephalus sechellensis*). *Mol. Ecol.* **10**: 2263–2273.

Schneider, S., Kueffer, J.M., Roessli, D. & Excoffier, L. 1997. *ARLEQUIN, version 1.1: a Software for Population Genetic Data Analysis*. Genetics and Biometry Laboratory, University of Geneva, Switzerland.

Schroeder, J., Lourenço, P.M., Hooijmeijer, J.C.E.W., Both, C. & Piersma, T. 2009. A possible case of contemporary selection leading to a decrease in sexual plumage dimorphism in a grassland-breeding shorebird. *Behav. Ecol.* **20**: 797–807.

Schroeder, J., Lourenço, P.M., van der Velde, M., Hooijmeijer, J.C.E.W., Both, C. & Piersma, T. 2008. Sexual dimorphism in plumage and size in Black-tailed Godwits *Limosa limosa limosa*. *Ardea* **96**: 25–37.

Senner, N.R., Verhoeven, M.A., Abad-Gómez, J.M., Alves, J.A., Hooijmeijer, J.C.E.W., Howison, R.A., Kentie, R., Loonstra, A.H.J., Masero, J.A., Rocha, A., Stager, M. & Piersma, T. 2019. High migratory survival and highly variable migratory behavior in Black-tailed Godwits. *Front. Ecol. Evol.* **7**: 96.

Sundberg, P. 1989. Shape and size – constrained principal components analysis. *Syst. Zool.* **38**: 166–168.

Tajima, F. & Nei, M. 1984. Estimation of evolutionary distance between nucleotide sequences. *Mol. Biol. Evol.* **11**: 22–31.

Trimbos, K.B., Doorenweerd, C., Kraaijeveld, K., Musters, C.J., Groen, N.M., de Knijff, P., Piersma, T. & de Snoo, G.R. 2014. Patterns in nuclear and mitochondrial DNA reveal historical and recent isolation in the Black-tailed Godwit (*Limosa limosa*). *PLoS One* **9**: e83949.

Tukey, J.W. 1949. Comparing individual means in the analysis of variance. *Biometrics* **5**: 99–114.

van der Velde, M., Haddrath, O., Verkuil, Y.I., Baker, A.J. & Piersma, T. 2017. New primers for molecular sex identification of waders. *Wader Study* **124**: 147–151.

Verhoeven, M.A., Loonstra, A.H.J., Senner, N.R., McBride, A.D., Both, C. & Piersma, T. 2019. Variation from an unknown source: large inter-individual differences in migrating Black-tailed Godwits. *Front. Ecol. Evol.* **7**: 31.

Wenink, P.W., Baker, A.J. & Tilanus, M.G. 1994. Mitochondrial control-control region sequences in two shorebird species, the Turnstone and the Dunlin, and their utility in population genetic studies. *Mol. Biol. Evol.* **11**: 22–31.

Zhu, B.R., Hassell, C.J., Verkuil, Y.I., Gunnarson, T.G., Hooijmeijer, J.C.E.W., Zhang, Z.-W. & Piersma, T. 2020. Size, shape and sex differences in three subspecies of Black-tailed Godwits *Limosa limosa*. *Bird Study* **67**: 45–52.

Received 23 January 2020;
revision accepted 21 September 2020.
Associate Editor: Bowie Rauri

SUPPORTING INFORMATION

Additional supporting information may be found online in the Supporting Information section at the end of the article.

Figure S1. Neighbor-joining phylogenetic tree based on sampling locations. The outgroup is Bar-tailed Godwit *Limosa lapponica*. Numbers indicate node support values from 1,000 bootstrap iterations.

Table S1. Banding information of Black-tailed Godwits from Iceland (*L. l. islandica*), The Netherlands (*L. l. limosa*), NW Australia (*L. l. melanuroides*) and Bohai Bay.

Table S2. Details of populations sampled for DNA (*n*: sample size, nh: number of haplotypes).

Table S3. Details of primers tested in Black-tailed Godwits to sequence the mitochondrial control region.

Table S4. Morphometrics and degree of sexual dimorphism (DSD) of Black-tailed Godwits from Iceland (*L. l. islandica*), The Netherlands (*L. l. limosa*), NW Australia (*L. l. melanuroides*) and Bohai Bay (Results are means ± sd).

Table S5. IDs, localities, subspecies and GenBank accession numbers of 195 individuals sequenced for the mtDNA control region.